Guo *et al.*
European Journal of Medical Research (2025) 30:306
https://doi.org/10.1186/s40001-025-02440-7

European Journal of Medical Research

RESEARCH Open Access

SAP30 promotes clear cell renal cell carcinoma proliferation and inhibits apoptosis through the MT1G axis

Wei Guo[1†], Shuwen Wang[1†], Zitong Yang[1†], Yu Dong[1], Zhinan Xia[1], Wei Xue[2*] and Cheng Zhang[1*]

Abstract

Sin3A-associated protein 30 (SAP30) is a crucial component of the SIN/HDAC histone deacetylase complex and acts as a scaffold that facilitates target gene binding. SAP30 is highly expressed in various tumours; however, its role in renal cell carcinoma (RCC) remains unclear. In our study, we observed the upregulation of SAP30 in clear cell renal cell carcinoma (ccRCC) tissues, and its elevated expression was correlated with a poor prognosis. Previous research has suggested that SAP30 may influence the growth, proliferation, and apoptosis of RCC cells. Gene Ontology (GO) analysis of the downstream regulatory targets of SAP30 revealed that SAP30 suppressed the expression of MT1G, a protein that binds to p53. Mechanistically, SAP30 inhibited MT1G transcription, thereby impairing the function of MT1G in delivering zinc ions to p53, which diminished p53 activity. Moreover, reduced MT1G levels attenuated the inhibitory effect of MT1G on MDM2, further destabilizing p53. Consequently, this cascade promoted RCC progression. In conclusion, our findings indicate that SAP30 inhibits the p53 pathway through MT1G suppression, suggesting that SAP30 and MT1G are potential prognostic markers and therapeutic targets for RCC.

Keywords Transcription factor, p53, SAP30, MT1G, ccRCC

Introduction

Renal cell carcinoma (RCC) is one of the most prevalent malignancies affecting the urinary system and accounts for approximately 5% of all cancer cases [1]. Among all RCC subtypes, clear cell renal cell carcinoma is the most predominant, accounting for more than 90% of all cases [2]. While surgery remains the primary treatment option for early-stage clear cell renal cell carcinoma (ccRCC), more than 30% of patients have already developed distant metastases by the time of diagnosis. Furthermore, postoperative survival rates are not particularly satisfactory [3, 4]. Additionally, the poor prognosis of clear cell renal cell carcinoma (ccRCC) is closely associated with resistance to radiotherapy and chemotherapy, as well as with the absence of effective biomarkers [5]. Therefore, finding suitable biomarkers is highly important.

Sin3A-associated protein 30 (SAP30) is a crucial component of the SIN/HDAC histone deacetylase complex. SAP30 is widely expressed in human tissues, particularly in hematopoietic tissues [6], and its functions primarily as a transcriptional repressor [7]. SAP30 acts as a scaffold for SIN3, which functions as a repressor and corepressor of gene expression in conjunction with binding proteins [8, 9]. SAP30 biological functions include the regulation of DNA and histonemethylation, nucleosome

[†]Wei Guo, Shuwen Wang and Zitong Yang have contributed equally.

*Correspondence:
Wei Xue
doctorxue@hrbmu.edu.cn
Cheng Zhang
zhangcheng13836182568@zju.edu.cn
[1] Department of Urology, Center for Oncology Medicine, the Fourth Affiliated Hospital of School of Medicine, and International School of Medicine, International Institutes of Medicine, Zhejiang University, Yiwu 322000, China
[2] Department of Urology, Shengjing Hospital of China Medical University, Shenyang 110004, China

remodeling, scaffolding for histonedeacetylases, and regulation of N-acetylglucosamine transferase activity [9]. SAP30 primarily achieves transcriptional repression through two mechanisms. First, SAP30 binds to transcription factors such as YY1 and recruits HDAC1, thereby facilitating transcriptional repression [10, 11]. Second, SAP30 directly binds to DNA sequences, inducing structural bending that contributes to transcriptional inhibition [12]. The knockout of SAP30 in yeast has been shown to produce effects similar to those observed when SIN3 and Rpd3 were knocked out. These proteins are involved in diverse functions,including cell cycle regulation, apoptosis, mitochondrial metabolism, and DNA replication and repair [6, 13–15]. Therefore, it can be inferred that the knockdown of SAP30 may also influence cell cycle regulation and apoptosis [16]. However, SAP30 has been minimally studied in various tumors; particularly, its mechanism of action in the onset and progression of ccRCC remains unclear.

Herein, we demonstrated that SAP30 suppressed the expression of metallothionein-1G (MT1G) at the transcriptional level. MT1G is a small cysteine-rich protein that is crucial for metal homeostasis, protection against heavy metal toxicity, DNA damage, and oxidative stress [17]. MT1G is expressed in various tumours and plays roles in cell growth, proliferation, and the epithelial–mesenchymal transition (EMT) process [18, 19]. MT1G increases the stability of p53 by inhibiting its ubiquitin ligase, MDM2 [20]. MT1G can also directly interact with p53 to supply zinc ions, thereby increasing p53 transcriptional activity [20]. However, MT1G has been relatively underexplored in the context of kidney cancer.

In this study, we demonstrated that SAP30 influenced the proliferation and apoptosis of kidney cancer cells through the MT1G/p53 axis both in vivo and in vitro. This molecular mechanism holds promise as a novel clinical therapeutic target for kidney cancer and deserves further investigation.

Methods and materials

Cell lines, cell culture and tissue specimens

Human renal cancer cell lines (786-O, CAKI-1, OS-RC-2, and CAKI-2) and human renal tubular epithelial cells (HK-2) were obtained from the Cell Resources Center, Shanghai Academy of Life Sciences, Chinese Academy of Sciences. The cell lines were cultured in the recommended media (RPMI-1640 Medium), supplemented with 10% heat-inactivated fetal bovine serum (Gibco, Beijing, China) and 1% streptomycin/penicillin (Keygen, Nanjing, China), at 37 °C in an atmosphere containing 5% CO2. Renal cell carcinoma (RCC) tissue samples were collected from 40 patients who underwent radical nephrectomy or kidney-sparing surgery at the Department of Urology, The First Affiliated Hospital of Harbin Medical University, between 2010 and 2019. All diagnoses were confirmed through histopathological examination.

Antibodies and reagents

The following antibodies were used for western blotting: anti-SAP30 (#LS-C676447, LSBio, Seattle, USA), anti-MT1G (#323,730, US Biological, Massachusetts, USA), anti-p53 (#60,283-2-Ig, Proteintech, Wuhan, China), anti-Bax (#50,599-2-Ig, Proteintech, Wuhan, China), anti-Bcl2 (#12,789-AP, Proteintech, Wuhan, China), anti-CCNB1 (#28,603-AP, Proteintech, Wuhan, China), anti-CCND1 (#60,186-I-Ig, Proteintech, Wuhan, China), and anti-CCNL2 (#LS-C749918, LSBio, Seattle, USA). The anti-SAP30 antibody for IHC was purchased from LSBio (#LS-C676447, Seattle, USA). The anti-SAP30 antibody used for ChIP–PCR was purchased from Abcam (#ab231804, Shanghai, China). Sunitinib was purchased from MCE (#HY-10255A, Shanghai, China).

siRNA and plasmid transfection

The siRNAs for SAP30 and MT1G were purchased from GenePharma (Suzhou, China), and their sequences are shown in Supplementary Table S1. Transfection of the siRNA-SAP30 and siRNA-MT1G vectors was performed with jetPRIME (Polyplus, Shanghai, China). The plasmids pENTER-SAP30, pENTER-NC, pCMV3-SAP30 and pCMV3-NC were purchased from Weizhen (Shandong, China) and Sino Biological (Beijing, China). Briefly, $1.2–1.3\times10^6$ cells were seeded in a 6-cm culture dish for transfection, and the cells were collected for subsequent experiments after 47–72 h.

Quantitative real-time PCR (qRT–PCR)

Total RNA from cells and tissues was extracted with the TRIzol reagent (Ambion, USA). A reverse transcription kit (TianGen, Beijing, China) and a SYBR Green PCR kit (TianGen, Beijing, China) were used to perform RT–qPCR according to the manufacturer's instructions. The sequences of the primers used are provided in Supplementary Table S1. The results were analysed via the 2-ΔΔCt method to quantify the fold changes.

Western blot analysis and immunohistochemical (IHC) staining

Proteins from nude mouse kidney cancer cells, tissues, and tumour cell lines were extracted with RIPA buffer (Beyotime, Shanghai, China) supplemented with protease inhibitors. The quantified proteins were separated by SDS–PAGE and transferred onto PVDF membranes. The membranes were subsequently blocked with 5%

BSA for 2 h at room temperature and then probed with appropriate antibodies. For immunohistochemistry (IHC), 4-μm-thick paraffin-embedded sections of kidney cancer tissue were deparaffinized, subjected to antigen retrieval, and blocked with 5% bovine serum albumin (BSA) for 2 h at room temperature. The sections were then incubated overnight at 4 °C with the antibody against SAP30 (dilution 1:400). On the following day, a peroxidase-conjugated polymer was applied for 30 min, followed by visualization with DAB (Beyotime, Shanghai, China).

CCK-8 cell proliferation assay

We utilized the CCK-8 assay (MCE, China) to assess cell proliferation. Transfected cells were seeded in 96-well plates at a density of 3000 cells per well and allowed to grow for 12 h. Subsequently, a 10% CCK-8 solution was added at various time points (0, 24, 48, and 72 h) following the manufacturers' instructions for the CCK-8 kit. The optical density (OD) values were measured at 450 nm via a 96-well plate reader.

Colony formation assay

The colony formation capacity of cells was evaluated via a plate colony formation assay. Transfected 786-O, CAKI-1, and OS-RC-2 cells were seeded at a density of 1×10^3 cells per well in 6-well plates and allowed to grow for 14 days to form colonies. The colonies were then fixed with paraformaldehyde and stained with crystal violet for visualization and quantification.

Hoechst staining

The apoptosis of the transfected cells was induced with H2O2. After fixation with paraformaldehyde, the cells were washed three times with PBS. The cells were subsequently stained with the Hoechst dye (#C1017, Beyotime, China) for 5 min and then photographed under a microscope.

Flow cytometry

Transfected cells were trypsinized with EDTA-free trypsin and washed with cold PBS according to the manufacturer's instructions for the Annexin V-FITC/PI apoptosis kit (Solarbio, Beijing, China). Then, the apoptosis was assessed by staining cells with Annexin V-FITC and Propidium Iodide (PI) in the dark. Finally, the cell cycle profiles were analyzed via PI staining and flow cytometry following the manufacturer's protocol for the cell cycle detection kit (Beyotime, Shanghai, China). Gating Strategy:

Cells were first gated using FSC/SSC parameters to exclude debris and identify intact populations. Apoptotic cells exhibited reduced FSC (cell shrinkage) and slightly increased SSC (chromatin condensation). Viability staining with PI distinguished live cells from necrotic/late apoptotic cells. A dual-parameter plot (Annexin V-FITC vs. PI) was used to classify four populations: Live cells (Annexin V^-/PI^-), Early apoptotic cells (Annexin V^+/PI^-), Late apoptotic cells (Annexin V^+/PI^+), Necrotic cells (Annexin V^-/PI^+). Color Compensation Strategy: Spectral spillover was calculated using single-color controls (unstained, Annexin V-FITC, PI, etc.) and corrected via a compensation matrix. PMT voltages were optimized to prevent signal saturation. Compensation accuracy was verified through quadrant alignment validation.

Chromatin immunoprecipitation (ChIP) assay

The chromatin immunoprecipitation assay with 786-O and CAKI-1 cells was performed according to the protocol for the SimpleChIP® Plus enzymatic chromatin IP kit with magnetic beads. First, 1×10^7 cells were fixed with 1% formaldehyde, and 1.25 M glycine was added to terminate the reaction. The cells were then washed with cold PBS containing a protease inhibitor and collected by centrifugation. Finally, the collected cells were sonicated in IP mixed medium and centrifuged at $14{,}000\times g$ for 30 min at 4 °C. Protein A/G agarose beads were mixed with the above supernatant and centrifuged, and the chromatin in the supernatant was immunoprecipitated overnight with antibodies against SAP30 or IgG. The protein A/G agarose beads were then washed with mixed wash buffer, LiCl/detergent, and TE buffer. The beads were heated overnight at 65 °C in a buffer mixture containing 1% SDS and 0.1 M NaHCO3 to reverse cross-link the beads. The beads were then treated with 1 ml of RNase A for 15 min at 37 °C and digested with 2 ml of a proteinase K solution for 1 h at 37 °C. Finally, the DNA was purified via extraction with LiCl, phenol/chloroform and ethanol, and the specific MT1G promoter region was amplified with a DNA template. Supplementary Table S1 lists the primer sequences designed to detect specific promoters.

Luciferase reporter assay

The SAP30-overexpressing plasmid pcDNA3.3-SAP30 and the plasmid pGL4.18WT + binding sites (BS1, BS2 and BS3) containing the promoter region of MT1G were constructed. The binding site sequences used for promoter reporter plasmid construction are listed in Supplementary Table S1. 293 T cells cultured in 6-well plates were transfected with the overexpression plasmids or empty vectors. Luciferase activity was measured via a

dual-luciferase reporter system (E1910, Promega, USA) according to the manufacturer's instructions.

Detection of EdU incorporation

Cells (3×10^5 cells/well) were seeded on coverslips in 6-well plates for 24 h. The cells were then cultured in a culture medium containing EdU for 2 h after 48 h of transfection. The cultures were subsequently stained with azide 488 and Hoechst 33,342. EdU-positive cells were observed under a fluorescence microscope and photographed. The EdU binding rate was expressed as the ratio of the number of EdU-positive (green) cells to the total number of Hoechst-stained(blue) cells.

Immunofluorescence (IF)

Cells (3×10^5 cells/well) were inoculated in 6-well plates with coverslips for 24 h. Thereafter, the cells were washed twice with PBS, fixed with 4% paraformaldehyde for 30 min, permeabilized with 0.05% Triton for 30 min, blocked with 5% BSA for 2 h, and incubated with an antibody against SAP30 overnight at 4 °C. On the next day, the slides were incubated with a type A fluorescent secondary antibody for 1 h at room temperature. Finally, nuclear staining was performed with DAPI, and subsequent imaging was performed via fluorescence microscopy.

Xenograft tumour growth

786-O cells (3×10^7 cells/ml) were injected into the posterior ventral sides of 6-week-old male nude mice obtained from Charles River Laboratories (Beijing, China). After 6 days, when the tumours became visible, their volumes were measured; afterwards, transfection was performed according to the instructions of the EntransterTM in vivo kit (EnGreen, Beijing, China) and repeated every 3 days. Forty-eight days later, the nude mice were sacrificed, the tumours were removed, and their weights and volumes were measured. The procedure adhered to the guidelines set by the Animal Ethics Committee of Harbin Medical University.

Statistical analysis

Statistical analysis was performed with the GraphPad software (version 7.0). The data are presented as the means ± standard deviations (SDs). Statistical significance was assessed via a t test, with $p<0.05$ considered significant.

Results

SAP30 is highly expressed in ccRCC cells and tissues and is correlated with an unfavourable prognosis

Transcription factors play crucial roles in regulating the development of cancer [21, 22]. Therefore, we initially intersected the differentially expressed genes from The Cancer Genome Atlas (TCGA) renal cancer dataset and the transcription factor ENCODE database to identify SAP30 as a potential transcriptional suppressor (Fig. 1A). SAP30 was found to be highly expressed in kidney renal clear cell carcinoma (KIRC) based on the TCGA data (Fig. 1B). Next, we evaluated the mRNA and protein expression levels of SAP30 in human clear cell renal cell carcinoma (ccRCC) samples from our study group. The PCR results revealed that SAP30 expression was greater in tumour tissue than in normal tissue in 34 pairs of samples (Fig. 1C) and was greater in the renal cancer cell lines than in normal renal tubular cells (HK-2) (Fig. 1D). Additionally, the western blotting results indicated that SAP30 expression was higher in the kidney cancer cell lines than in HK-2 cells (Fig. 1E). To further validate the differential expression of SAP30 in ccRCC, we performed immunohistochemical (IHC) staining on 40 pairs of tumour and adjacent noncancerous tissues. SAP30 was significantly upregulated in tumour tissues compared with adjacent nontumour tissues (Fig. 1F, G). Finally, we found that high SAP30 expression was associated with shorter overall survival (OS) times of ccRCC patients from the TCGA dataset (Fig. 1H). In summary, SAP30 is highly expressed in ccRCC and is correlated with a poor prognosis.

SAP30 knockdown inhibits ccRCC cell proliferation and promotes cell apoptosis

To assess the biological significance of SAP30 in ccRCC, we used specific siRNAs to knock down SAP30 expression in three different ccRCC cell lines (786-O, CAKI-1,

(See figure on next page.)

Fig. 1 SAP30 is highly expressed in ccRCC and is highly correlated with the patient prognosis. **A** Venn diagram showing shared genes between the upregulated differentially expressed genes in the KIRC TCGA dataset (|log2FC|> 2; *p value < 0.05) and transcription factors in the ENCODE database. **B** Data on the SAP30 expression were obtained and plotted from the TCGA database (|log2FC| cut-off: 1; *p value < 0.01). **C** SAP30 mRNA expression in 34 pairs of ccRCC samples, shown as the mean ± SD. Statistical analysis was conducted via a t test (*p < 0.05). **D** mRNA expression of SAP30 in 5 cell lines. **E** Protein expression of SAP30 in 5 cell lines. **F**–**G** Immunohistochemical verification of SAP30 protein levels in 40 pairs of cancer and adjacent nontumour tissues. **H** Kaplan–Meier curve of overall survival (OS) of patients in the TCGA cohort according to SAP30 expression

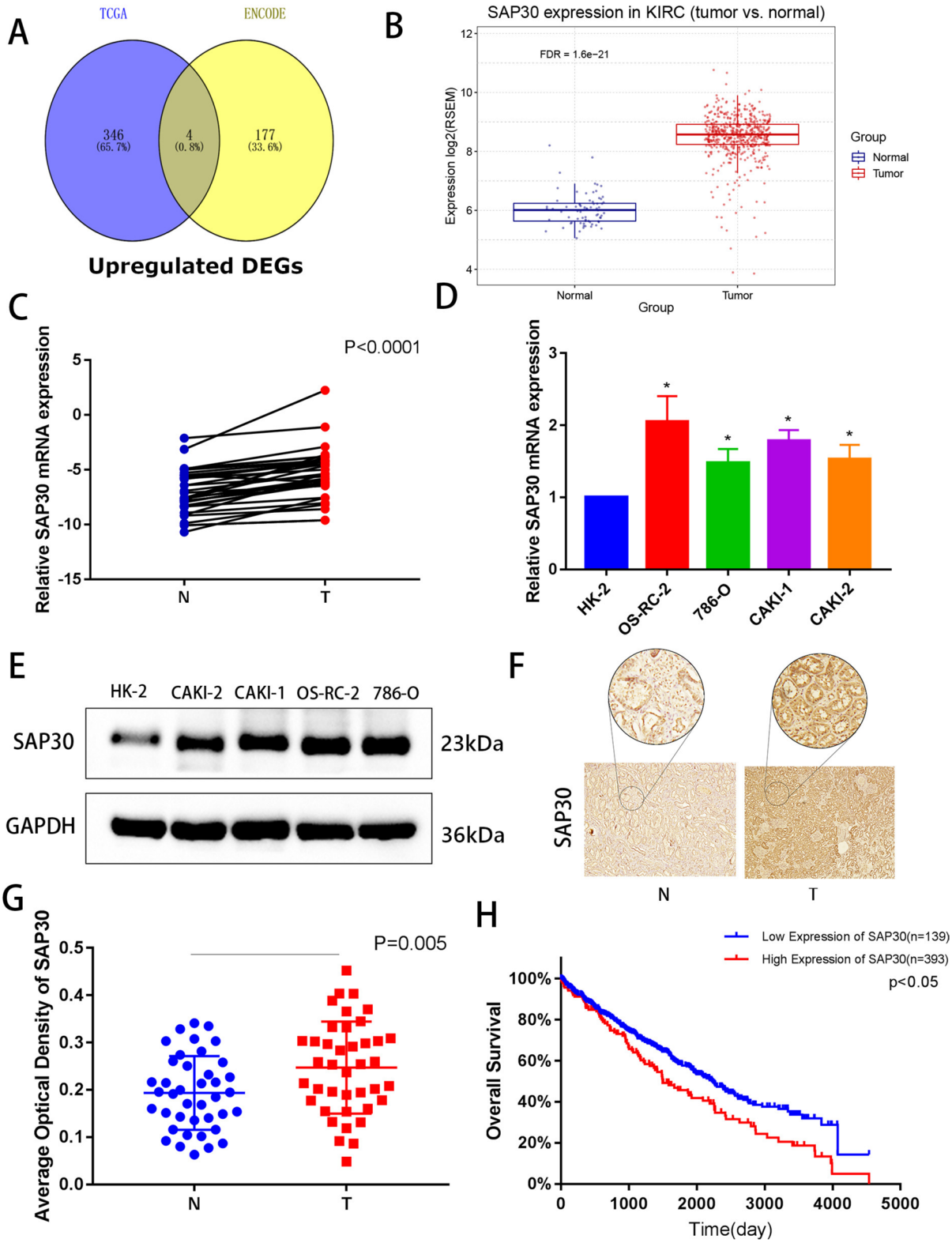

Fig. 1 (See legend on previous page.)

and OS-RC-2) (Fig. 2A, B). The results of the CCK-8 assay demonstrated that the knockdown of SAP30 inhibited the proliferation of all the three tumour cell lines tested (Fig. 2C). Consistently, the inhibition of proliferation was further evidenced by the decreased colony formation upon SAP30 gene silencing in ccRCC cells (Fig. 2D, E). We hypothesized that SAP30 might influence cell viability by affecting apoptosis. Consistent with this hypothesis, Hoechst staining revealed that SAP30 knockdown promoted cell apoptosis (Fig. 2F, G). Moreover, flow cytometry was used to detect apoptosis, and the cell cycle assay revealed that the knockdown of SAP30 increased cell apoptosis (Fig. 2H, I) and blocked the G1 to G2 phase transition (Fig. 2J, K) in the three cell lines. Based on the aforementioned effects on the phenotypes, we also evaluated changes in the levels of apoptosis- and cell cycle-related proteins following SAP30 knockdown. Upon SAP30 gene silencing in the three cell lines, the expression of cell cycle-related proteins, such as CCNB1, CCND1, and CCNL2, was significantly downregulated (Fig. 2L). Additionally, SAP30 knockdown increased the expression of the proapoptotic protein Bax and decreased the expression of the antiapoptotic protein Bcl2 (Fig. 2M). Importantly, we found that the p53 protein expression increased upon SAP30 knockdown (Fig. 2M), indicating that SAP30 may be a key factor affecting cell proliferation and apoptosis [23]. Thus, these data suggest that SAP30 may promote cell proliferation, inhibit apoptosis, and affect cell cycle arrest by potentially modulating the p53 signalling pathway in ccRCC.

Overexpression of SAP30 promotes ccRCC cell proliferation and inhibits cell apoptosis

In addition, SAP30-overexpressing (SAP30-OE) constructs were transfected into 786-O and CAKI-1 cells to ectopically increase SAP30 expression (Fig. 3A, B). The CCK-8 and EdU assays demonstrated that the overexpression of SAP30 promoted the proliferation of renal cancer cells (Fig. 3C–E), and flow cytometry confirmed that the overexpression of SAP30 also inhibited cell apoptosis (Fig. 3F, G). Additionally, the overexpression of SAP30 reduced the proportion of cells in the G1 phase of the cell cycle (Fig. 3H, I). These results indicate that the overexpression of SAP30 promotes the proliferation and inhibits the apoptosis of tumour cells.

SAP30 affects the proliferation and apoptosis of tumour cells through the MT1G/p53 pathway in ccRCC

The Sin3 histone deacetylase (HDAC) complex is a typical co-repressor complex, a multi-protein complex recruited to chromatin by DNA-binding repressor proteins to facilitate local histone deacetylation and transcriptional repression [24]. To determine the mechanism by which SAP30 contributes to the observed phenotypes, we identified 251 potential targets by intersecting the putative targets of SAP30 from the ENCODE database with the genes differentially expressed in kidney cancer from the TCGA database (Fig. 4A). Gene Ontology (GO) term analysis was subsequently conducted on the 251 target genes. Among them, metallothionein, which is associated with growth-related functions, attracted our attention (Fig. 4B). Studies have shown that MT1G can interact with p53 to promote its expression in hepatocellular carcinoma [20], and therefore, we hypothesized that MT1G and p53 could be involved in the mechanism by which SAP30 affects the proliferation and apoptosis in ccRCC. Subsequent western blot analysis revealed increased protein expression of MT1G and p53 following the knockdown of SAP30 in the 786-O and CAKI-1 cell lines (Fig. 4C). Next, we simultaneously knocked down MT1G and SAP30 and observed that knocking down MT1G reversed the effect of SAP30 silencing on p53 protein levels (Fig. 4C). These results suggest that SAP30 regulates the expression of the p53 protein through MT1G. Indeed, the CCK-8 and colony formation assays demonstrated that the knockdown of MT1G restored the tumour cell viability by partially reversing the inhibitory effect of SAP30 silencing on tumour cell growth (Fig. 4D–F). We subsequently used flow cytometry and observed that the knockdown of MT1G partially restored the number of cells undergoing apoptosis, which was induced as a result of SAP30 silencing (Fig. 4G, H). These findings suggest that SAP30 influences the proliferation and the apoptotic phenotype

(See figure on next page.)

Fig. 2 SAP30 knockdown inhibits the proliferation and promotes the apoptosis of tumour cells. **A** Protein expression of SAP30 in the si-Ctrl, si-SAP30-1 and si-SAP30-2 groups. **B** mRNA expression of SAP30 in the si-Ctrl, si-SAP30-1 and si-SAP30-2 groups. **C**–**E** CCK-8 and colony formation assays were performed to analyse the effect of si-SAP30 on the proliferation of 786-O, CAKI-1 and OS-RC-2 cells. **F**, **G** The numbers of apoptotic cells detected by Hoechst staining in the si-Ctrl and si-SAP30 groups; the arrows indicate apoptotic cells. **H**–**K** Flow cytometry was used to detect cell apoptosis and determine the cell cycle phase in the si-Ctrl and si-SAP30 groups of 786-O, CAKI-1 and OS-RC-2 cells. **L** Expression levels of cell cycle-related proteins in SAP30-knockdown 786-O, CAKI-1 and OS-RC-2 cells. **M** Expression levels of apoptosis-related proteins in SAP30-knockdown 786-O, CAKI-1 and OS-RC-2 cells. *$p < 0.05$, **$p < 0.01$, ***$p < 0.001$

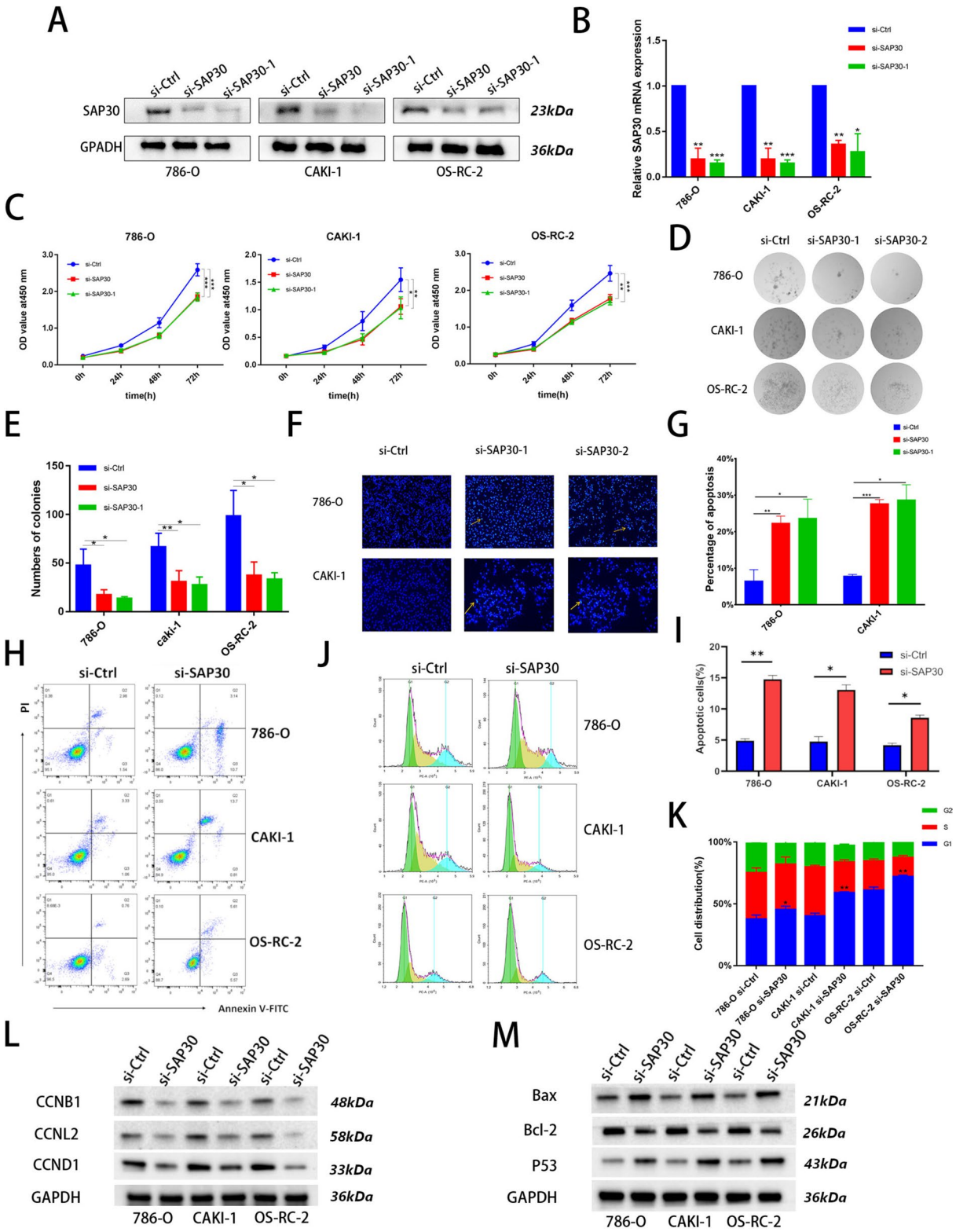

Fig. 2 (See legend on previous page.)

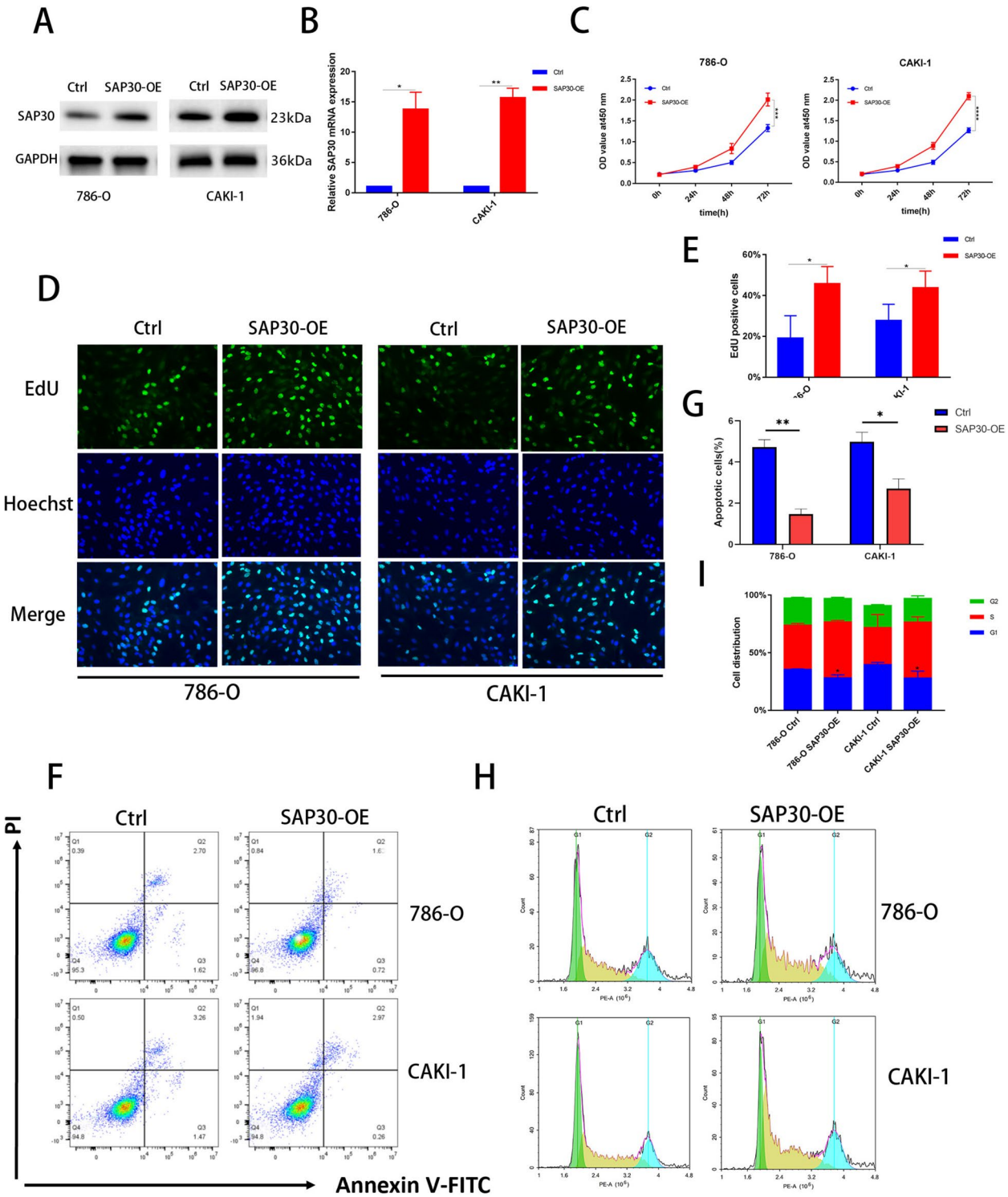

Fig. 3 Overexpression of SAP30 promotes the proliferation and inhibits the apoptosis of tumour cells. **A**, **B** Protein and mRNA expression of SAP30 in the Ctrl and SAP30-OE groups. **C**–**E** CCK-8 and EdU (green: EdU positive) assays were used to analyse the effects of SAP30-OE on the proliferation of 786-O and CAKI-1 cells. **F**–**I** Flow cytometry was used to detect cell apoptosis and cell cycle progression in the Ctrl and SAP30-OE groups of 786-O and CAKI-1 cells. *p < 0.05, **p < 0.01, ***p < 0.001

of kidney cancer cells primarily by modulating the p53 protein through its interaction with MT1G.

SAP30, as a transcription repressor, binds to the promoter of MT1G to inhibit its transcription

Given that SAP30 functions as a transcriptional repressor, we used immunofluorescence microscopy to examine SAP30 protein localization and observed its predominant localization in the nucleus (Fig. 5A). We subsequently analysed the expression levels of MT1G in ccRCC by using data from the TCGA database, and interestingly, MT1G was found to be significantly downregulated in ccRCC (Fig. 5B). However, analysis of the TCGA database did not confirm a significant correlation between DNA methylation of MT1G and its low expression in renal cancer (Fig. 5C). Because SAP30 is a component of the histone deacetylation complex and because MT1G is reportedly induced by histone deacetylase inhibitor (HDACi) treatment [19], the low expression of MT1G in renal cancer may be due to the regulation of deacetylation. We speculated that either knocking down SAP30 or using a histone deacetylase inhibitor (HDACi) has the potential to increase MT1G protein and mRNA expression (Fig. 5D, E). To further validate the correlation between SAP30 levels and those of MT1G and p53 in clinical samples, we assessed their expression in 40 tumour samples via IHC (Fig. 5F), which revealed that SAP30 expression was significantly negatively correlated with MT1G and p53 expression (Fig. 5G, H). These findings suggest that SAP30 suppresses MT1G expression at the transcriptional level. Furthermore, a luciferase reporter assay demonstrated that SAP30 inhibited MT1G gene transcription at binding site 1, which is GGAGCTCTCAG (Fig. 5I). Next, to assess the ability of SAP30 to bind to the MT1G promoter region, a chromatin immunoprecipitation (ChIP) assay was conducted. The results demonstrated that SAP30 knockdown reduced its binding to the MT1G promoter (Fig. 5J). The positions of the SAP30 binding sites are marked with coloured boxes (Fig. 5K). In summary, the data indicate that SAP30 binds to the MT1G promoter region, leading to negative regulation of MT1G transcription and influencing downstream gene expression.

SAP30 knockdown suppressed tumour growth in a ccRCC xenograft mouse model

The effect of SAP30 on ccRCC development was further validated in vivo via a xenograft mouse model. 786-O cells were subcutaneously injected into the flanks of nude mice (Fig. 6A, B). Once the tumours became clearly visible, their sizes were measured every three days. The mice were then sacrificed, and the tumour weight and volume were recorded. Compared with those in the si-ctrl group, the volume and weight of the tumours in the SAP30-knockdown group were significantly lower, but this reduction was reversed by the knockdown of MT1G (Fig. 6C–E). Notably, the regulation of MT1G and p53 expression by SAP30 was confirmed again in vivo. Consistent with the in vitro results, RT–PCR and western blot analysis revealed that the expression of MT1G and p53 was significantly increased following SAP30 knockdown (Fig. 6F, G). These in vivo experiments further demonstrated that inhibiting SAP30 expression in ccRCC could suppress tumour progression by upregulating MT1G and p53.

Discussion

The high mortality rate of patients with renal cell carcinoma (RCC) is primarily attributable to challenges like early diagnosis, postoperative tumor recurrence, high metastasis rates, and radiotherapy resistance. Therefore, it is crucial to explore effective molecular biological treatment targets [25]. Genetic regulation relies heavily on transcription factors [26], which play important roles in various diseases, including cancer [21, 27]. The Cancer Dependency Map (DepMap) project has highlighted the critical roles of transcription factors in tumor development and maintenance, suggesting their potential as therapeutic target [28]. Previous studies have identified SAP30 as a biomarker for various tumors, including hepatocellular carcinoma, renal cell carcinoma, and basal cell carcinoma [29–31]. However, the biological function and mechanism of action of SAP30 remain poorly understood. In our study, SAP30 was highly expressed in

(See figure on next page.)

Fig. 4 SAP30 knockdown promotes the expression of the MT1G and p53 proteins, while MT1G knockdown reverses the alterations in p53 protein levels, cell proliferation and apoptosis-related phenotypes caused by the knockdown of SAP30. **A** Venn diagram showing shared genes between the downregulated differentially expressed genes in the KIRC TCGA dataset (|log2FC|> 2; *p value < 0.05) and transcription factors in the ENCODE database. **B** The top 30 enriched GO terms for 251 genes. **C** Protein expression of p53 and MT1G in the si-Ctrl, si-SAP30, si-MT1G and si-S + M groups. **D**–**F** CCK-8 and colony formation assays were used to analyse the effects of si-Ctrl, si-SAP30, si-MT1G and si-S + M on the proliferation of 786-O and CAKI-1 cells. **G**, **H** Flow cytometry was used to detect apoptosis in the si-Ctrl, si-SAP30, si-MT1G and si-S + M groups of 786-O and CAKI-1 cells. *p < 0.05, **p < 0.01, ***p < 0.001

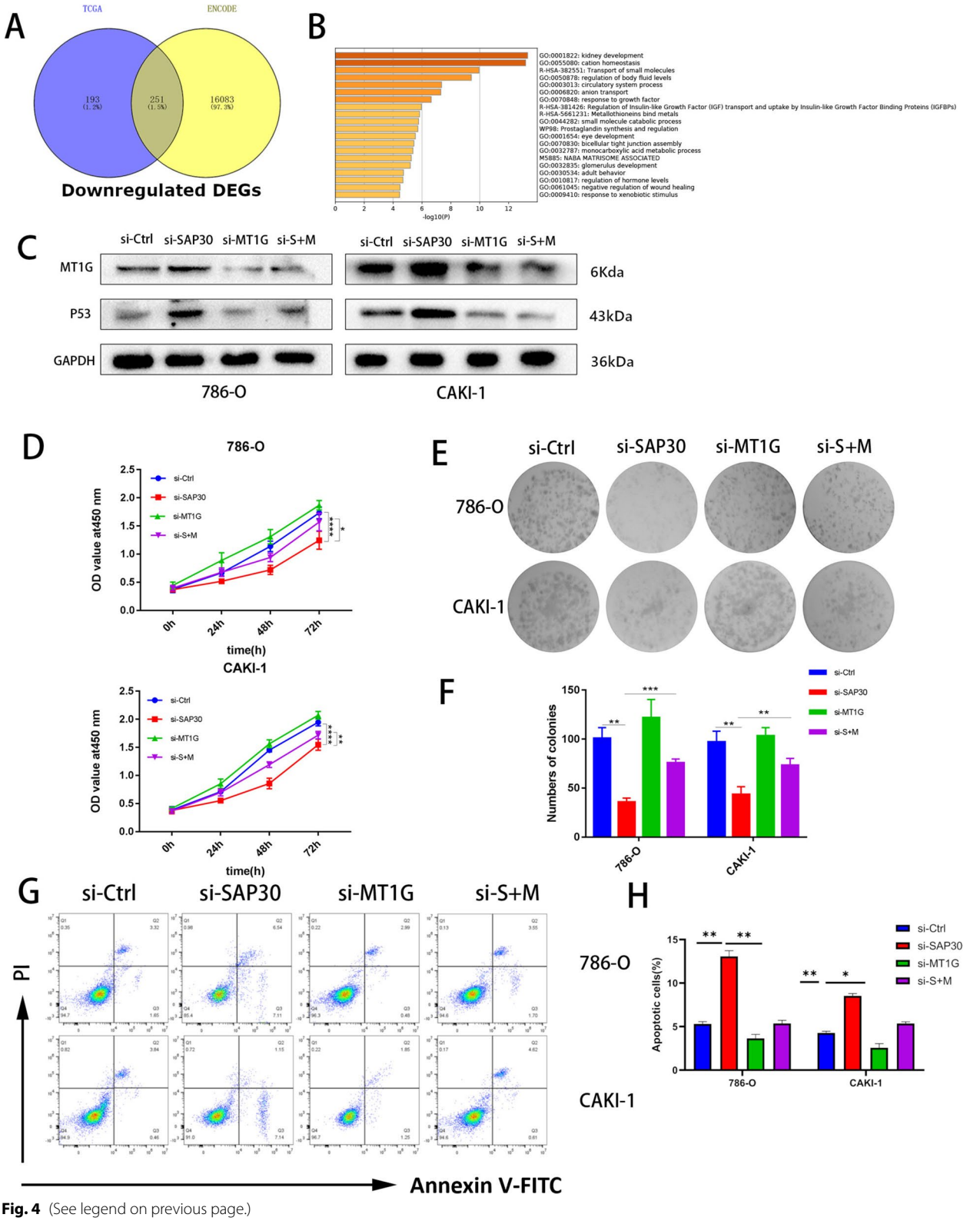

Fig. 4 (See legend on previous page.)

ccRCC tissues based on data from TCGA. And this finding was corroborated using our own samples, confirming elevated SAP30 levels at both mRNA and protein levels in ccRCC tissues. Furthermore, high SAP30 expression was associated with poor patient prognosis. Through detailed cell experiments and an in vivo mouse model, we demonstrated that SAP30 plays a pivotal role in promoting apoptosis in kidney cancer cells. Additionally, we found that SAP30 inhibits the p53 pathway. Overall, our data suggest that SAP30 facilitates the development of ccRCC and could be a potential therapeutic target for this disease.

To further explore the mechanism by which SAP30 promotes renal cancer cell growth and inhibits apoptosis, we used the ENCODE and TCGA databases to identify the downstream targets of SAP30. We performed GO analysis of the identified target gene set, which indicated that MT1G might serve as a bridge between SAP30 and its effects on renal cancer cell proliferation and apoptosis. A dual-luciferase reporter assay and ChIPPCR confirmed that SAP30 suppresses MT1G transcription. The role of MT1G in stabilizing and activating p53 has been validated in hepatocellular carcinoma (HCC) [20]. We found that SAP30 affected p53 expression via MT1G. Our findings indicate that the SAP30/MT1G/p53 signaling axis plays a significant role in SAP30-induced proliferation and inhibition of apoptosis in ccRCC. However, our data analysis did not identify which HDAC family members are recruited by SAP30 to repress the transcription of MT1G. Additionally, our analysis cannot exclude the possibility that other signaling pathways of SAP30 in ccRCC operate in parallel with the SAP30/MT1G/p53 axis. These limitations require further experiments. Small-molecule inhibitors are a significant treatment option for advanced renal cancer [32].

MT1G, a member of the metallothionein family, is one of the eight functional isoforms of MT1 and a small cysteine-rich protein [17]. MT1G has been studied in liver, prostate, esophageal, and pancreatic cancers and is closely associated with ferroptosis, drug resistance, cell proliferation and apoptosis, and tumor cell stemness [33–36]. However, limited evidence has linked MT1G to kidney cancer. In our study, we found low expression of MT1G in ccRCC. MT1G knockdown restored the inhibition of SAP30-induced apoptosis and proliferation induced by SAP30 knockdown in both cell lines and a mouse model. Studies have indicated that MT1G was essential for the SAP30-mediated regulation of tumour cell growth and apoptosis, collectively influencing ccRCC development. Given that SAP30 is a component of the histone deacetylase complex, we demonstrated that HDAC inhibitors could also reduce MT1G expression at the mRNA and protein levels in kidney cancer cell lines. These findings suggest that low MT1G expression in kidney cancer is at least partly regulated by histone deacetylation. Previous reports have shown that low MT1G expression in kidney cancer is not significantly correlated with methylation [37], supporting our conclusions. Further research should explore whether other factors mediate the low expression of MT1G in kidney cancer.

The TP53 gene encodes the p53 protein, which has anticancer effects. During cancer suppression, p53 binds to DNA response elements to induce various biological activities, including cell cycle arrest, apoptosis, DNA repair, autophagy, and ferroptosis [38–40]. Because p53 is a zinc ion-dependent transcription factor [41] and the p53 ubiquitinate MDM2 can affect its stability [42], knocking down SAP30 upregulated the p53 protein level, and this upregulation was partially reversed by knocking down MT1G. However, we cannot completely rule out that SAP30 affects p53 in other ways. Overall, our results suggest that p53 collaborates with SAP30 and MT1G in regulating ccRCC development.

Taken together, our findings highlight the critical role of SAP30 knockdown in inhibiting cell proliferation and enhancing apoptosis to impede ccRCC progression. Our results also demonstrated that the SAP30/MT1G/p53 axis affects the proliferation and apoptosis of ccRCC cells both in vitro and in vivo, suggesting that this axis may be a future therapeutic target for ccRCC.

Conclusion

In summary, our study demonstrated that the transcriptional repressor SAP30 promoted the proliferation and inhibited the apoptosis of ccRCC cells through the MT1G/p53 pathway. SAP30 could bind to the

(See figure on next page.)

Fig. 5 SAP30 binds to the MT1G promoter region to repress MT1G expression. **A** Immunofluorescence was used to determine the location of SAP30 in 786-O and CAKI-1 cells. **B** The MT1G mRNA expression data were obtained from TCGA. **C** Spearman correlation between MT1G methylation and mRNA expression in the KIRC TCGA dataset. **D**, **E** mRNA and protein levels of MT1G were determined in the si-Ctrl, si-SAP30 and HDACi groups. **F** Immunohistochemical staining for the SAP30, MT1G and p53 proteins in tumour tissues. **G**, **H** Correlations between the levels of SAP30 and MT1G and p53 were analysed. **I** Dual-luciferase reporter assay results showing the activity of the MT1G promoter fragment. **J** ChIP–PCR analysis of the binding of SAP30 to the MT1G promoter. **K** Binding site base pair sequences are indicated with boxes. *$p < 0.05$, **$p < 0.01$, ***$p < 0.001$

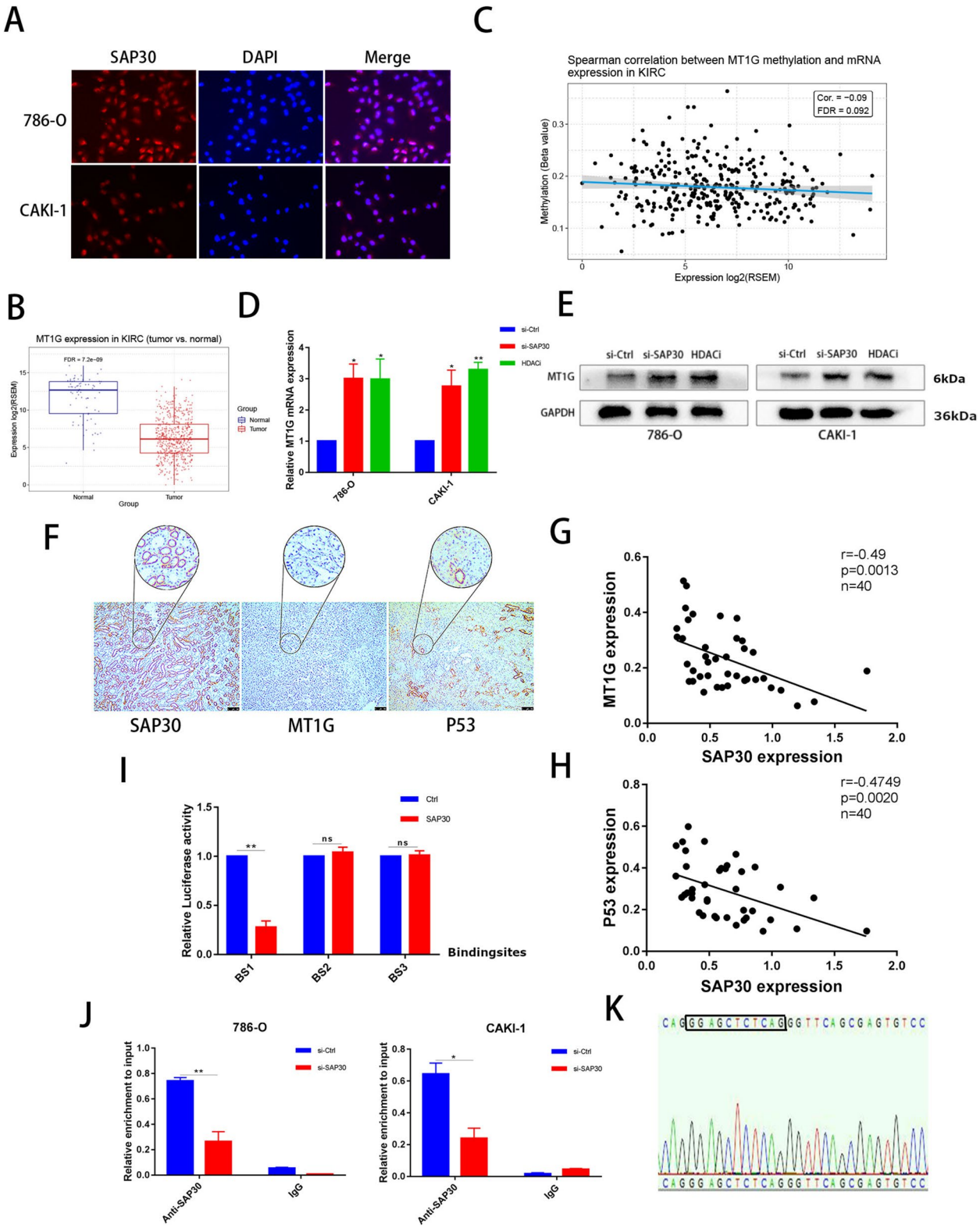

Fig. 5 (See legend on previous page.)

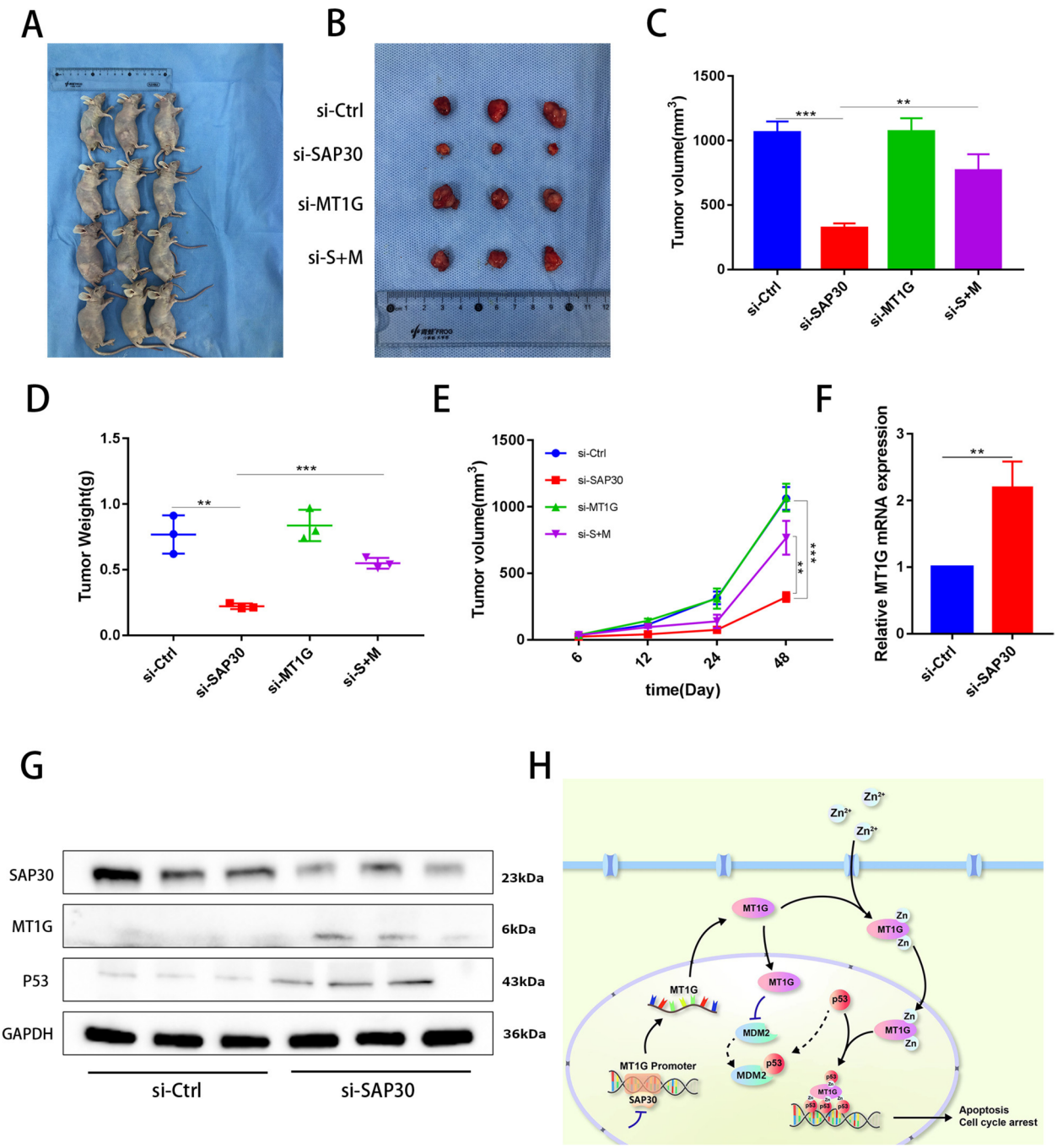

Fig. 6 SAP30 knockdown inhibits ccRCC progression in vivo. **A**, **B** The subcutaneous tumours in 12 nude mice and the isolated tumours are shown. **C**, **D** The volumes and weights of the tumours were measured in nude mice. **E** The tumour volumes were measured at 6, 12, 24 and 48 days after tumour formation. **F** MT1G mRNA expression was measured by qRT–PCR in the si-Ctrl and si-SAP30 groups in vivo. **G** The protein expression levels of SAP30, MT1G and p53 were determined in the si-Ctrl and si-SAP30 groups in vivo. **H** Hypothetical model of the proposed mechanism by which SAP30 regulates the proliferation and apoptosis of ccRCC cells through the MT1G/p53 axis. *p < 0.05, **p < 0.01, ***p < 0.001

MT1G promoter region, repressing MT1G expression at the transcriptional level. This reduced the interaction between MT1G and p53, leading to decreased p53 protein levels by promoting MDM2-mediated p53 degradation. Ultimately, SAP30 promotes tumour cell proliferation and inhibits tumour cell apoptosis.

Supplementary Information

The online version contains supplementary material available at https://doi.org/10.1186/s40001-025-02440-7.

Supplementary material 1.

Acknowledgements
The original draft was prepared and written by Wei Guo. Shuwen Wang was responsible for the data processing. Zitong Yang and Yu Dong helped review and revise all the diagrams, and Zhinan Xia helped review and revise the article. Wei Xue and Cheng Zhang designed the experiments and managed the project. All the authors contributed to the article and approved the submitted version.

Author contributions
The original draft was prepared and written by Wei Guo. Shuwen Wang was responsible for the data processing. Zitong Yang and Yu Dong helped review and revise all the diagrams, and Zhinan Xia helped review and revise the article. Wei Xue and Cheng Zhang designed the experiments and managed the project. All the authors contributed to the article and approved the submitted version.

Funding
This study was funded in part by the National Natural Science Foundation of China (Grant No. 81872084).

Availability of data and materials
No datasets were generated or analysed during the current study.

Declarations

Ethics approval and consent to participate
This study was conducted at the Department of Urology, The First Affiliated Hospital of Harbin Medical University, Harbin, Heilongjiang Province, China. The study was authorized by the Institutional Review Board of Harbin Medical University, and the patients provided informed consent for this study.

Consent for publication
Not applicable.

Competing interests
The authors declare no competing interests.

Received: 9 October 2024 Accepted: 7 March 2025
Published online: 18 April 2025

References:

1. Siegel RL, Miller KD, Jemal A. Cancer statistics, 2020. CA Cancer J Clin. 2020;70(1):7–30. https://doi.org/10.3322/caac.21590.
2. Hsieh JJ, Purdue MP, Signoretti S, et al. Renal cell carcinoma. Nat Rev Dis Primers. 2017;3:17009. https://doi.org/10.1038/nrdp.2017.9.
3. Koul H, Huh JS, Rove KO, et al. Molecular aspects of renal cell carcinoma: a review. Am J Cancer Res. 2011;1(2):240–54.
4. Sánchez-Gastaldo A, Kempf E, González Del Alba A, Duran I. Systemic treatment of renal cell cancer: a comprehensive review. Cancer Treat Rev. 2017;60:77–89. https://doi.org/10.1016/j.ctrv.2017.08.010.
5. van der Mijn JC, Mier JW, Broxterman HJ, Verheul HM. Predictive biomarkers in renal cell cancer: insights in drug resistance mechanisms. Drug Resist Updat. 2014;17(4–6):77–88. https://doi.org/10.1016/j.drup.2014.10.003.
6. Zhang Y, Sun ZW, Iratni R, et al. SAP30, a novel protein conserved between human and yeast, is a component of a histone deacetylase complex. Mol Cell. 1998;1(7):1021–31. https://doi.org/10.1016/s1097-2765(00)80102-1.
7. Silverstein RA, Ekwall K. Sin3: a flexible regulator of global gene expression and genome stability. Curr Genet. 2005;47(1):1–17. https://doi.org/10.1007/s00294-004-0541-5.
8. Zhang Y, Iratni R, Erdjument-Bromage H, Tempst P, Reinberg D. Histone deacetylases and SAP18, a novel polypeptide, are components of a human Sin3 complex. Cell. 1997;89(3):357–64. https://doi.org/10.1016/s0092-8674(00)80216-0.
9. Grzenda A, Lomberk G, Zhang JS, Urrutia R. Sin3: master scaffold and transcriptional corepressor. Biochim Biophys Acta. 2009;1789(6–8):443–50. https://doi.org/10.1016/j.bbagrm.2009.05.007.
10. Huang NE, Lin CH, Lin YS, Yu WC. Modulation of YY1 activity by SAP30. Biochem Biophys Res Commun. 2003;306(1):267–75. https://doi.org/10.1016/s0006-291x(03)00966-5.
11. Le May N, Mansuroglu Z, Léger P, et al. A SAP30 complex inhibits IFN-beta expression in Rift Valley fever virus infected cells. PLoS Pathog. 2008;4(1):e13. https://doi.org/10.1371/journal.ppat.0040013.
12. Viiri KM, Jänis J, Siggers T, et al. DNA-binding and -bending activities of SAP30L and SAP30 are mediated by a zinc-dependent module and monophosphoinositides. Mol Cell Biol. 2009;29(2):342–56. https://doi.org/10.1128/MCB.01213-08.
13. Bernstein BE, Tong JK, Schreiber SL. Genomewide studies of histone deacetylase function in yeast. Proc Natl Acad Sci U S A. 2000;97(25):13708–13. https://doi.org/10.1073/pnas.250477697.
14. Sun ZW, Hampsey M. A general requirement for the Sin3-Rpd3 histone deacetylase complex in regulating silencing in Saccharomyces cerevisiae. Genetics. 1999;152(3):921–32. https://doi.org/10.1093/genetics/152.3.921.
15. Loewith R, Smith JS, Meijer M, et al. Pho23 is associated with the Rpd3 histone deacetylase and is required for its normal function in regulation of gene expression and silencing in Saccharomyces cerevisiae. J Biol Chem. 2001;276(26):24068–74. https://doi.org/10.1074/jbc.M102176200.
16. He Y, Imhoff R, Sahu A, Radhakrishnan I. Solution structure of a novel zinc finger motif in the SAP30 polypeptide of the Sin3 corepressor complex and its potential role in nucleic acid recognition. Nucleic Acids Res. 2009;37(7):2142–52. https://doi.org/10.1093/nar/gkp051.
17. Si M, Lang J. The roles of metallothioneins in carcinogenesis. J Hematol Oncol. 2018;11(1):107. https://doi.org/10.1186/s13045-018-0645-x.
18. Joshi B, Ordonez-Ercan D, Dasgupta P, Chellappan S. Induction of human metallothionein 1G promoter by VEGF and heavy metals: differential involvement of E2F and metal transcription factors. Oncogene. 2005;24(13):2204–17. https://doi.org/10.1038/sj.onc.1208206.
19. Fu J, Lv H, Guan H, et al. Metallothionein 1G functions as a tumor suppressor in thyroid cancer through modulating the PI3K/Akt signaling pathway. BMC Cancer. 2013;13:462. https://doi.org/10.1186/1471-2407-13-462.
20. Wang Y, Wang G, Tan X, et al. MT1G serves as a tumor suppressor in hepatocellular carcinoma by interacting with p53. Oncogenesis. 2019;8(12):67. https://doi.org/10.1038/s41389-019-0176-5.
21. Bushweller JH. Targeting transcription factors in cancer - from undruggable to reality. Nat Rev Cancer. 2019;19(11):611–24. https://doi.org/10.1038/s41568-019-0196-7.
22. Lambert M, Jambon S, Depauw S, David-Cordonnier MH. Targeting transcription factors for cancer treatment. Molecules. 2018;23(6):1479. https://doi.org/10.3390/molecules23061479.
23. Dannenberg JH, David G, Zhong S, van der Torre J, Wong WH, Depinho RA. mSin3A corepressor regulates diverse transcriptional networks governing normal and neoplastic growth and survival. Genes Dev. 2005;19(13):1581–95. https://doi.org/10.1101/gad.1286905.
24. Adams GE, et al. Co-repressor, co-activator and general transcription factor: the many faces of the Sin3 histone deacetylase (HDAC) complex. Biochem J. 2018;475(24):3921–32. https://doi.org/10.1042/BCJ20170314.
25. Capitanio U, Montorsi F. Renal cancer. Lancet. 2016;387(10021):894–906. https://doi.org/10.1016/S0140-6736(15)00046-X.

26. Lambert SA, Jolma A, Campitelli LF, et al. The human transcription factors. Cell. 2018;172(4):650–65. https://doi.org/10.1016/j.cell.2018.01.029.
27. Nishioka H, Inoshita N. New WHO classification of pituitary adenomas (4th edition): assessment of pituitary transcription factors and the prognostic histological factors. Brain Tumor Pathol. 2018;35(2):57–61. https://doi.org/10.1007/s10014-017-0307-7.
28. Tsherniak A, Vazquez F, Montgomery PG, et al. Defining a cancer dependency map. Cell. 2017;170(3):564-576.e16. https://doi.org/10.1016/j.cell.2017.06.010.
29. Snezhkina AV, Nyushko KM, Zaretsky AR, et al. Transcription factor SAP30 is involved in the activation of NETO2 gene expression in clear cell renal cell carcinoma. Mol Biol. 2018;52(3):451–9. https://doi.org/10.7868/S0026898418030072.
30. Sironi E, Cerri A, Tomasini D, et al. Loss of heterozygosity on chromosome 4q32-35 in sporadic basal cell carcinomas: evidence for the involvement of p33ING2/ING1L and SAP30 genes. J Cutan Pathol. 2004;31(4):318–22. https://doi.org/10.1111/j.0303-6987.2004.0187.x.
31. Chen Z, Zou Y, Zhang Y, et al. A novel prognostic signature based on four glycolysis-related genes predicts survival and clinical risk of hepatocellular carcinoma. J Clin Lab Anal. 2021;35(11): e24005. https://doi.org/10.1002/jcla.24005.
32. Barata PC, Rini BI. Treatment of renal cell carcinoma: current status and future directions. CA Cancer J Clin. 2017;67(6):507–24. https://doi.org/10.3322/caac.21411.
33. Liu H, Gao L, Xie T, Li J, Zhai TS, Xu Y. Identification and validation of a prognostic signature for prostate cancer based on ferroptosis-related genes. Front Oncol. 2021;11:623313. https://doi.org/10.3389/fonc.2021.623313.
34. Sun X, Niu X, Chen R, et al. Metallothionein-1G facilitates sorafenib resistance through inhibition of ferroptosis. Hepatology. 2016;64(2):488–500. https://doi.org/10.1002/hep.28574.
35. Zhu L, Yang F, Wang L, et al. Identification the ferroptosis-related gene signature in patients with esophageal adenocarcinoma. Cancer Cell Int. 2021;21(1):124. https://doi.org/10.1186/s12935-021-01821-2.
36. Li K, Zhang Z, Mei Y, et al. Metallothionein-1G suppresses pancreatic cancer cell stemness by limiting activin A secretion via NF-κB inhibition. Theranostics. 2021;11(7):3196–212. https://doi.org/10.7150/thno.51976.
37. Maleckaite R, Zalimas A, Bakavicius A, Jankevicius F, Jarmalaite S, Daniunaite K. DNA methylation of metallothionein genes is associated with the clinical features of renal cell carcinoma. Oncol Rep. 2019;41(6):3535–44. https://doi.org/10.3892/or.2019.7109.
38. Hafner A, Bulyk ML, Jambhekar A, Lahav G. The multiple mechanisms that regulate p53 activity and cell fate. Nat Rev Mol Cell Biol. 2019;20(4):199–210. https://doi.org/10.1038/s41580-019-0110-x.
39. Levine AJ. The many faces of p53: something for everyone. J Mol Cell Biol. 2019;11(7):524–30. https://doi.org/10.1093/jmcb/mjz026.
40. Janic A, Valente LJ, Wakefield MJ, et al. DNA repair processes are critical mediators of p53-dependent tumor suppression. Nat Med. 2018;24(7):947–53. https://doi.org/10.1038/s41591-018-0043-5.
41. Méplan C, Richard MJ, Hainaut P. Metalloregulation of the tumor suppressor protein p53: zinc mediates the renaturation of p53 after exposure to metal chelators in vitro and in intact cells. Oncogene. 2000;19(46):5227–36. https://doi.org/10.1038/sj.onc.1203907.
42. Pant V, Aryal NK, Xiong S, Chau GP, Fowlkes NW, Lozano G. Alterations of the Mdm2 C-terminus differentially impact its function in vivo. Cancer Res. 2022;82(7):1313–20. https://doi.org/10.1158/0008-5472.CAN-21-2381.

Publisher's Note